Syntheses and Crystal Structures of New Quaternary Ag-Containing Group 5 Chalcogenides: $KAg_2M^VSe_4$ and $K_3Ag_3M^V{}_2S_8$ (M^V = Nb, Ta)

Wen-Tong Chen,[1,2] **Hong-Wei Ma,**[1] **Guo-Cong Guo,**[*,1] **Lei Deng,**[1] **Guo-Wei Zhou,**[1]
Zhen-Chao Dong,[3] **and Jin-Shun Huang**[1]

[1]State Key Laboratory of Structural Chemistry, Fujian Institute of Research on the Structure of matter, the Chinese Academy of Sciences, Fuzhou, Fujian 350002, P. R. China

[2]Graduate School, the Chinese Academy of Sciences, Beijing 100039, P. R. China

[3]National Institute for Materials Science, 1-2-1 Sengen, Tsukuba, Ibaraki 305-0047

Received July 23, 2003; E-mail: gcguo@ms.fjirsm.ac.cn

Four new quaternary Ag-containing group 5 chalcogenides, KAg_2NbSe_4 (**1**), KAg_2TaSe_4 (**2**), $K_3Ag_3Nb_2S_8$ (**3**), and $K_3Ag_3Ta_2S_8$ (**4**), have been prepared through the use of molten alkali metal polychalcogenides as reactive fluxes and structurally characterized by single-crystal X-ray diffraction techniques. The layer-type structures of **1** and **2** can be regarded as constructed from the basic building block of the incomplete cubane $[Ag_3M^VSe_3]$, which are corner-shared to form an infinite chain along the *a* direction. These incomplete cubane chains are interconnected and further bridged by Se atoms along the *c* direction, leading to a two-dimensional structure. The crystal structure of **3** and **4** consists of one-dimensional triple-metal $[Ag_3M^V{}_2S_8]^{3-}$ anionic chains seperated by K^+ cations. The alternate packing of M^VS_4 and AgS_4 tetrahedra via edge-sharing along the *b* direction leads to mixed-metal sub-chains, every two of which are further linked by AgS_4 tetrahedra along the *a* direction through edge-sharing to the M^VS_4 tetrahedra, thus yielding the so-called triple-metal chains.

Metal chalcogenides are of long standing interest because of their useful properties. In particular, group 5 chalcogenides have been investigated extensively in regards to their superconductivity and charge density wave transition properties.[1] Quaternary group 5 chalcogenides $A/M^I/M^V/Q$ (A = alkali metal; M^I = Cu, Ag; M^V = V, Nb, Ta; Q = S, Se, Te) that have been isolated and structurally characterized are mainly copper compounds, e.g., $A_2CuM^VQ_4$,[2] $ACu_2M^VQ_4$,[3] $K_3Cu_3M^V{}_2Q_8$ (M^V = Nb, Ta; Q = S, Se),[4] $K_3CuNb_2Se_{12}$,[2b] and $Na_8Cu_4Nb_2S_{21}$.[5] In contrast, the examples of silver analogues are limited, amounting only to the $A_2M^IM^VQ_4$ structure type, such as A_2AgVQ_4,[6] A_2AgNbQ_4,[6b,7] and A_2AgTaQ_4.[7b]

The quaternary group 5 chalcogenides are now generally prepared by the reactive flux method first described by Ibers.[8] This technique has been well established as a new route for the preparation of new compounds containing (poly)chalcogenide species.[9] Due to the propensity of copper atoms to assume an oxidation state of I, copper was usually employed as a pseudoalkali metal to substitute for the K^+ ions in $K_3M^VQ_4$ (M^V = V, Nb, Ta; Q = S, Se, Te).[10,2d] Because of the different coordination preference between Cu and K cations, the dimensionality of the resulting compounds increases with the decrease in alkali metal content.[11] This trend has also been found in a new series of metal chalcogenides $K_2M^IM^{III}{}_3Se_6$.[12] The scarcity of quaternary silver analogues stimulated our interests in the metal chalcogenides.[13]

In this paper we report the syntheses and structural characterizations of new quaternary silver group 5 chalcogenides, $KAg_2M^VSe_4$ and $K_3Ag_3M^V{}_2S_8$ (M = Nb, Ta), prepared by the reactive flux technique, which, to our knowledge, are the first silver compounds to form $AM^I{}_2M^VQ_4$ and $A_3M^I{}_3M^V{}_2Q_8$ type structures.

Experimental

Materials. All materials were of analytical grade and used as received.

Syntheses. KAg_2MSe_4 (M = Nb (**1**), Ta (**2**)) were prepared from the reaction of K_2Se_4 (0.394 g, 1 mmol), Nb (0.093 g, 1 mmol) or Ta (0.181 g, 1 mmol), Ag (0.108 g, 1 mmol), and Se (0.395 g, 5 mmol). K_2Se_4 was made from the stoichiometric reaction of elemental K and Se in liquid ammonia under a nitrogen atmosphere. The starting materials were loaded into a Pyrex tube that was subsequently evacuated to 10^{-4} Torr and flame-sealed. The tubes were placed in a programmable furnace, slowly heated from room temperature to 450 °C at a rate of 2 °C/h, kept at 450 °C for a week, slowly cooled to 150 °C at 4 °C/h, and finally cooled to room temperature over 4 h. The excess K_xSe_y flux was removed by washing with DMF to isolate orange prismatic crystals of KAg_2MSe_4 in low yield (ca. 10% on Ag powder).

$K_3Ag_3M_2S_8$ (M = Nb (**3**), Ta (**4**)) compounds were synthesized from a similar reaction of K_2S_4 (0.207 g, 1 mmol), powders of elemental Nb (0.093 g, 1 mmol) or Ta (0.181 g, 1 mmol), Ag (0.108 g, 1 mmol), and S (0.160 g, 5 mmol). K_2S_4 was made from the stoichiometric reaction of elemental K with S in liquid ammonia under a nitrogen atmosphere. The tubes were placed in a furnace that was slowly heated from room temperature to 500 °C over 24 h and held there for a week, afterwards cooled to 475 °C at 1 °C/h, then to 150 °C at 4 °C/h, and finally to room temperature over 4 h. The excess K_xS_y flux was removed by washing with DMF to isolate dark-brown prismatic crystals of $K_3Ag_3M_2S_8$ in low yield (ca. 10% on Ag powder).

Published on the web March 12, 2004; DOI 10.1246/bcsj.77.505

X-ray Crystallographic Study. Crystals mounted inside 0.5 mm Lindemann glass capillaries were used for data collection on a Rigaku RAXISCS3 diffractometer for **1** and **2**, and on a Rigaku AFC5R diffractometer for **3** and **4** using graphite-monochromated Mo-Kα radiation ($\lambda = 0.71073$ Å) from a rotating anode generator. For **3** and **4**, the data sets were collected using the ω–2θ scan technique and corrected for Lorentz and polarization effects and absorption based on the ψ-scan. All structures were solved by direct methods and refined by full-matrix least squares on F^2 using the SHELXTL™ software package for crystallography.[14] All atoms were refined anisotropically. A summary of crystallographic data and structure analyses are listed in Table 1, and selected bond distances and angles are given in Table 2.

Results and Discussion

The layer-type structure of $KAg_2M^VSe_4$ (M^V = Nb (**1**), Ta (**2**)) can be viewed as constructed from the basic building block of incomplete cubane [Ag_3NbSe_3]. The incomplete cubanes are condensed into an infinite chain along the *a* direction through corner-sharing of Ag2 atoms. These incomplete cubane chains are interconnected and further bridged by Se1 and Se2 atoms along the *c* direction, leading to a two-dimensional structure, as shown in Fig. 1. Both the Ag and M^V atoms are tetrahedrally coordinated by Se atoms with the Nb–Se distances ranging from 2.382(2) to 2.454(1) Å [average Nb–Se: 2.426(2) Å] for **1** and the Ta–Se distances from 2.395(1) to 2.458(1) Å [average

Table 1. Summary of Crystallographic Data and Structure Analysis for **1**–**4**

Compound	**1**	**2**	**3**	**4**
Formula	KAg_2NbSe_4	KAg_2TaSe_4	$K_3Ag_3Nb_2S_8$	$K_3Ag_3Ta_2S_8$
Fw	663.59	751.63	883.21	1059.29
Crystal size/mm^3	0.20 0.20 0.15	0.30 0.15 0.15	0.25 0.10 0.10	0.35 0.15 0.15
Crystal system	orthorhombic	orthorhombic	monoclinic	monoclinic
Space group	*Ama*2 (No. 40)	*Ama*2 (No. 40)	$C2/c$ (No. 15)	$C2/c$ (No. 15)
a/Å	7.741(2)	7.810(2)	23.638(7)	23.598(3)
b/Å	19.024(4)	19.004(4)	5.544(2)	5.589(2)
c/Å	5.694(1)	5.730(1)	14.290(6)	14.307(5)
β/°	90	90	121.14(7)	120.63(2)
V/Å^3	838.5(3)	850.5(3)	1603(1)	1623.7(8)
Z	4	4	4	4
$2\theta_{max}$/°	50	50	50	50
Reflections collected	1152	1361	2527	1444
Independent, observed	687, 636	777, 738	1324, 1182	1409, 1097
Reflections/R_{int}	(0.0039)	(0.0385)	(0.0378)	(0.0281)
d_{calcd}/g cm^{-3}	5.257	5.870	3.660	4.333
μ/mm^{-1}	23.729	34.900	6.774	18.744
T/K	293(2)	293(2)	293(2)	293(2)
$F(000)$	1160	1288	1632	1888
$R1$, $wR2$[a)]	0.0363, 0.0962	0.0459, 0.1314	0.0544, 0.1629	0.0557, 0.1482
S	0.988	1.011	1.031	1.086
Largest and mean Δ/σ	0.001, 0	0, 0	0, 0	0.001, 0
$\Delta\rho$(max/min)/e Å^{-3}	0.724/−0.794	2.274/−2.405	1.331/−1.617	3.057/−2.727

a) $R1 = \Sigma||F_o| - |F_c||/\Sigma|F_o|$, $wR2 = \{\Sigma[w(F_o{}^2 - F_c{}^2)^2]/\Sigma[w(F_o{}^2)^2]\}^{1/2}$.

Table 2. Selected Bond Distances (Å) and Bond Angles (°) for **1**–**4**

Compound **1**			
Nb(1)–Ag(1)	2.712(1)	Ag(1)–Se(1)	2.552(1)
	2.982(1)	Ag(1)–Se(2)	2.546(2)
Nb(1)–Ag(2)	2.8587(6) ×2	Ag(1)–Se(3)	2.366(1) ×2
Nb(1)–Se(1)	2.454(1)	Ag(2)–Se(1)	2.4656(9) ×2
Nb(1)–Se(2)	2.382(2)	Ag(2)–Se(3)	2.435(1) ×2
Nb(1)–Se(3)	2.434(1) ×2		
Se(2)–Nb(1)–Se(1)	110.28(6)	Se(3)–Ag(1)–Se(2)	110.12(3) ×2
Se(3)–Nb(1)–Se(1)	108.64(3) ×2	Se(3)–Ag(1)–Se(3)	113.59(6)
Se(2)–Nb(1)–Se(3)	110.18(4) ×2	Se(3)–Ag(2)–Se(3)	116.73(6)
Se(3)–Nb(1)–Se(3)	108.87(6)	Se(3)–Ag(2)–Se(1)	108.24(3) ×4
Se(2)–Ag(1)–Se(1)	102.22(6)	Se(1)–Ag(2)–Se(1)	103.54(5)
Se(3)–Ag(1)–Se(1)	110.10(3) ×2		

Continued on next page

Continued from the previous page

Compound **2**			
Ta(1)–Ag(1)	2.818(2)	Ag(1)–Se(1)	2.499(2)
	2.913(2)	Ag(1)–Se(2)	2.500(2)
Ta(1)–Ag(2)	2.8644(5) ×2	Ag(1)–Se(3)	2.431(2) ×2
Ta(1)–Se(1)	2.450(1)	Ag(2)–Se(1)	2.453(1) ×2
Ta(1)–Se(2)	2.395(1)	Ag(2)–Se(3)	2.469(1) ×2
Ta(1)–Se(3)	2.458(1) ×2		
Se(2)–Ta(1)–Se(1)	109.88(4)	Se(3)–Ag(1)–Se(2)	109.41(4) ×2
Se(3)–Ta(1)–Se(1)	108.91(2) ×2	Se(3)–Ag(1)–Se(3)	110.5(1)
Se(2)–Ta(1)–Se(3)	110.20(3) ×2	Se(3)–Ag(2)–Se(3)	114.85(8)
Se(3)–Ta(1)–Se(3)	108.72(5)	Se(3)–Ag(2)–Se(1)	108.43(3) ×4
Se(2)–Ag(1)–Se(1)	104.98(9)	Se(1)–Ag(2)–Se(1)	105.58(8)
Se(3)–Ag(1)–Se(1)	111.18(4) ×2		
Compound **3**			
Ag(1)–Nb(1)	2.796(1) ×2	Ag(2)–S(3)	2.355(2)
Ag(2)–Nb(1)	2.768(1)	Ag(2)–S(4)	2.331(2)
	2.780(1)	Nb(1)–S(1)	2.308(2)
Ag(1)–S(1)	2.354(2) ×2	Nb(1)–S(2)	2.302(2)
Ag(1)–S(2)	2.352(2) ×2	Nb(1)–S(3)	2.290(2)
Ag(2)–S(1)	2.359(2)	Nb(1)–S(4)	2.259(2)
Ag(2)–S(2)	2.359(2)		
Nb(1)–Ag(1)–Nb(1)	179.22(4)	S(3)–Ag(2)–S(2)	110.13(6)
Nb(1)–Ag(2)–Nb(1)	175.96(3)	S(4)–Ag(2)–S(1)	115.65(6)
Ag(2)–Nb(1)–Ag(2)	175.96(3)	S(3)–Ag(2)–S(1)	104.77(6)
Ag(2)–Nb(1)–Ag(1)	88.43(2)	S(2)–Ag(2)–S(1)	115.25(5)
	87.66(2)	S(4)–Nb(1)–S(3)	110.01(5)
S(2)–Ag(1)–S(2)	111.66(7)	S(4)–Nb(1)–S(2)	108.45(7)
S(2)–Ag(1)–S(1)	104.62(5) ×2	S(3)–Nb(1)–S(2)	109.48(6)
	110.70(5) ×2	S(4)–Nb(1)–S(1)	112.41(6)
S(1)–Ag(1)–S(1)	114.71(8)	S(3)–Nb(1)–S(1)	108.63(5)
S(4)–Ag(2)–S(3)	106.61(6)	S(2)–Nb(1)–S(1)	107.80(5)
S(4)–Ag(2)–S(2)	104.17(7)		
Compound **4**			
Ag(1)–Ta(1)	2.7851(5) ×2	Ag(2)–S(3)	2.371(3)
Ag(2)–Ta(1)	2.792(2)	Ag(2)–S(4)	2.338(2)
	2.801(2)	Ta(1)–S(1)	2.308(2)
Ag(1)–S(1)	2.358(2) ×2	Ta(1)–S(2)	2.306(2)
Ag(1)–S(2)	2.372(3) ×2	Ta(1)–S(3)	2.280(2)
Ag(2)–S(1)	2.366(3)	Ta(1)–S(4)	2.261(2)
Ag(2)–S(2)	2.372(2)		
Ta(1)–Ag(1)–Ta(1)	179.09(6)	S(3)–Ag(2)–S(2)	109.42(9)
Ta(1)–Ag(2)–Ta(1)	176.03(5)	S(4)–Ag(2)–S(1)	116.56(8)
Ag(2)–Ta(1)–Ag(2)	176.03(5)	S(3)–Ag(2)–S(1)	103.75(9)
Ag(2)–Ta(1)–Ag(1)	88.66(4)	S(2)–Ag(2)–S(1)	115.88(9)
	87.76(4)	S(4)–Ta(1)–S(3)	110.00(8)
S(2)–Ag(1)–S(2)	111.2(1)	S(4)–Ta(1)–S(2)	108.10(8)
S(2)–Ag(1)–S(1)	110.57(7) ×2	S(3)–Ta(1)–S(2)	109.13(8)
	104.91(7) ×2	S(4)–Ta(1)–S(1)	112.22(8)
S(1)–Ag(1)–S(1)	114.9(1)	S(3)–Ta(1)–S(1)	108.62(9)
S(4)–Ag(2)–S(3)	107.51(9)	S(2)–Ta(1)–S(1)	108.72(8)
S(4)–Ag(2)–S(2)	103.45(8)		

Ta–Se: 2.440(1) Å] for **2**, which are comparable with those found in their respective copper analogues.[3d,3f,3g] The Se–M^{V}–Se angles in the present compounds show normal tetrahedral values. Interestingly, unlike the copper analogues in which the Cu–Se distances span over a narrow range, the Ag–Se distances are broadly distributed (2.366(1)–2.552(1) Å for **1** and

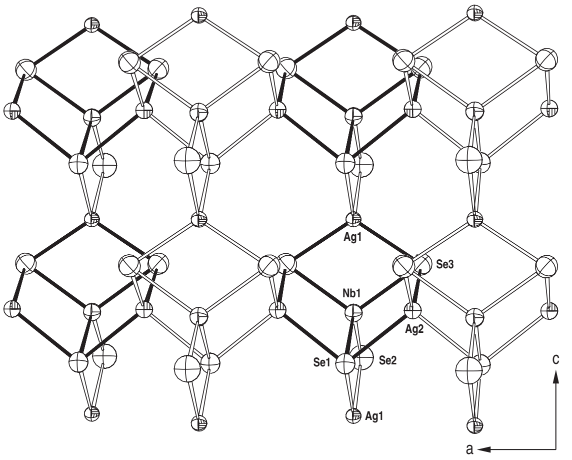

Fig. 1. Layered structure composed of incomplete cubanes in **1** viewed approximately along the *b* direction with 25% probability ellipsoids. For clarity, the bond shapes of incomplete cubanes are different.

2.431(2)–2.500(2) Å for **2**), which are obviously shorter than those found in the literature.[6b,7a] In addition, the crystallographically independent Ag atoms are both in a more distorted tetrahedral environment (Se–Ag–Se: 102.22(6)–116.73(6)° for **1**, 104.98(9)–114.85(8)° for **2**) with respect to the copper analogues. The mean Ag–Nb separation of 2.852(1) Å in **1** is about 0.2 Å shorter than those reported in the literature,[6b,7a] while the average Ag–Ta distance of 2.864(2) Å in **2** is about 0.1 Å shorter than those reported.[7b] The K^+ cations are located between the layers in **1** and **2** (Fig. 2).

The crystal structure of $K_3Ag_3M^VS_8$ (M = Nb (**3**), Ta (**4**)) consists of well-separated K^+ cations and one-dimensional chain $[Ag_3M^V{}_2S_8]^{3-}$ anions. The structure of the anionic chain can be viewed as follows: M^VS_4 and $Ag(2)S_4$ tetrahedra are edge-shared alternately along the *b* direction to form a mixed-metal sub-chain. Every two of such mixed-metal sub-chains are further linked by crystallographically independent $Ag(1)S_4$ tetrahedra along the *a* direction through edge-sharing of the M^VS_4 tetrahedra, thus yielding the so-called triple-metal chains, as shown in Fig. 3. The Nb–S distances in **3** range from 2.259(2) to 2.308(2) Å, comparing well with those in $K_3Cu_3Nb_2S_8$ (2.264(2) to 2.307(2) Å) and K_3NbS_4 (2.241(8) to 2.257(8) Å).[10a] The Ta–S distances in **4** range from 2.261(2) to 2.308(2) Å, comparable with those in the AgS_4 and TaS_4 tetrahedra of the edge-sharing compounds A_2AgTaS_4 (A = K, Rb, Cs)[7b] and K_3TaS_4.[10b] The Ag–S distances in **3** and **4** are comparable with each other, but are about 0.2 Å shorter than those in A_2AgTaS_4.[7b] Accordingly, the Ag–Ta distances are shortened by about 0.2 Å in comparison with those in A_2AgTaS_4.[7b] The K^+ cations in **3** and **4** are located between the triple-metal chains.

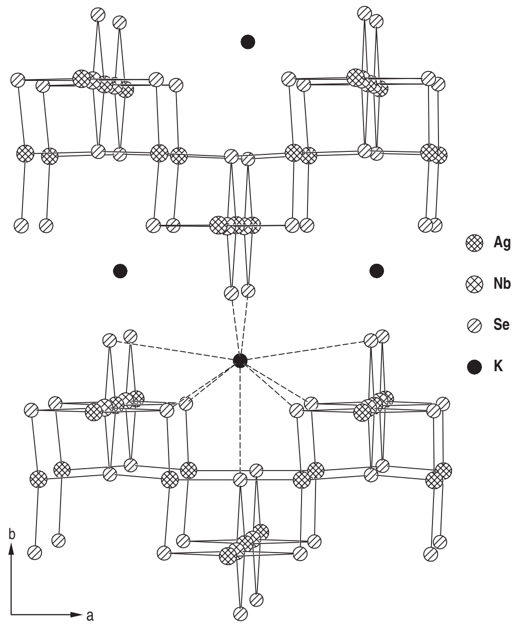

Fig. 2. Crystal structure of **1** shows the stacking of anionic layers and cations along the *b* direction. The atoms are different with shapes. Dashed lines represent the coordination environment of K cations.

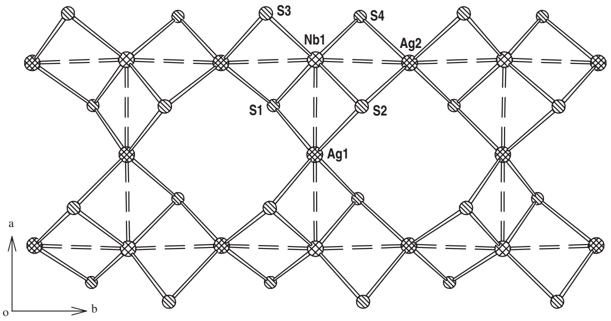

Fig. 3. Triple-metal chains in **3** extended along the *b* direction, dashed lines representing the Nb–Ag contacts.

The dimensionality of the structure of isolated $A_3M^VQ_4$ (expressed as $A_6M^V{}_2Q_8$, A = alkali metals, M^V = group 5 elements, Q = chalcogen) changes to single metal chain compounds $A_2M^IM^VQ_4$ (M^I = group 11 elements) when two of the six alkali metals are replaced by group 11 metals, to triple-metal chain compounds $A_3M^I{}_3M^V{}_2Q_8$ when three of the six alkali metals are replaced, to 2-D compounds $AM^I{}_2M^VQ_4$ when four of the six alkali metals are replaced, and to 3-D compounds $M^I{}_3M^VQ_4$ when all alkali metals are replaced. In the series of $A_{6-n}M^I{}_nM^V{}_2Q_8$ (n = 0–6), two types of compounds, $A_5M^IM^V{}_2Q_8$ and $AM^I{}_5M^V{}_2Q_8$, await future synthesis and structural characterization.

Table 3 summarizes the relationship between the Cu–Q bond distances and the substitution number of coinage metals for the copper analogs, which obviously shows that the M^I–Q bond distances in this substituted coinage metals $A_3M^VQ_4$ decrease with an increase in the substitution number of coinage metals. This trend should be due to the increasing dimensionality of the structure, as mentioned above, and result in the closer packing of compounds.

This work is supported by the National Natural Sciences Foundation of China (20001007, 20131020), Natural Sciences Foundation of the Chinese Academy of Sciences (KJCX2-H3) and Fujian Province (2000F006).

Table 3. The Relationship between the Cu–Q (Q = S, Se) Bond Distances and the Substitution Number of Coinage Metals for the Copper Analogs

Substitution number	Compounds	Cu–Q bond lengths/Å	Substitution number	Compounds	Cu–Q bond lengths/Å
2	K_2CuVS_4	2.313	2	K_2CuVSe_4	2.418
4	KCu_2VS_4	2.292–2.300	4	KCu_2VSe_4	2.390–2.402
6	Cu_3VS_4	2.298	2	$K_2CuNbSe_4$	2.457
2	K_2CuNbS_4	2.359	4	KCu_2NbSe_4	2.426–2.439
3	$K_3Cu_3Nb_2S_8$	2.333–2.360	2	$K_2CuTaSe_4$	2.456
4	$NaCu_2NbS_4$	2.319–2.342	4	KCu_2TaSe_4	2.430–2.441

Supplementary Materials. Figures S1–S5: the figures for compounds **2**–**4**. Further details of the crystal-structure investigations may be obtained from the Fachinformationszentrum Karlsruhe, D-76344 Eggenstein-Leopoldshafen, Germany, on quoting the depository numbers CSD-412479 (**1**), CSD-412477 (**2**), CSD-412478 (**3**), and CSD-412476 (**4**).

References

1 a) F. W. Boswell, J. C. Bennett, and A. Prodan, *J. Solid State Chem.*, **144**, 454 (1999). b) T. Ohtani, S. Honji, and M. Takano, *J. Solid State Chem.*, **132**, 188 (1997). c) N. Kijima, M. Takahashi, N. Matsumoto, and S. Nagata, *J. Solid State Chem.*, **135**, 325 (1998). d) M. Köckerling, D. Johrendt, and E. W. Finckh, *J. Am. Chem. Soc.*, **120**, 12297 (1998).

2 a) W. Bensch, P. Dürichen, and C. Weidlich, *Z. Kristallogr.*, **211**, 931 (1996). b) Y. J. Lu and J. A. Ibers, *Inorg. Chem.*, **30**, 3317 (1991). c) Y. J. Lu, P. Wu, and J. A. Ibers, *Eur. J. Solid State Inorg. Chem.*, **30**, 101 (1993). d) P. Dürichen and W. Bensch, *Eur. J. Solid State Inorg. Chem.*, **33**, 309 (1996). e) C. Rumpf, R. Tillinski, C. Näther, P. Dürichen, I. Jeß, and W. Bensch, *Eur. J. Solid State Inorg. Chem.*, **34**, 1187 (1997).

3 a) W. Bensch, P. Dürichen, and C. Weidlich, *Z. Kristallogr.*, **211**, 933 (1996). b) K. Peters, E. M. Peters, H. G. von Schnering, C. Mujica, G. Carvajal, and J. Llanos, *Z. Kristallogr.*, **211**, 812 (1996). c) C. Rumpf, C. Näther, I. Jeß, and W. Bensch, *Eur. J. Solid State Inorg. Chem.*, **34**, 1165 (1997). d) Y. J. Lu and J. A. Ibers, *J. Solid State Chem.*, **94**, 381 (1991). e) J. A. Cody, E. J. Wu, C. M. Cheung, and J. A. Ibers, *J. Solid State Chem.*, **121**, 225 (1996). f) Y. J. Lu and J. A. Ibers, *J. Solid State Chem.*, **107**, 58 (1993). g) Y. J. Lu and J. A. Ibers, *J. Solid State Chem.*, **111**, 447 (1994). h) J. Li, H. Y. Guo, D. M. Proserpio, and A. Sironi, *J. Solid State Chem.*, **117**, 247 (1995). i) J. A. Cody, E. J. Wu, C. M. Cheung, and J. A. Ibers, *J. Solid State Chem.*, **121**, 225 (1996).

4 Y. J. Lu and J. A. Ibers, *J. Solid State Chem.*, **98**, 312 (1992).

5 C. Rumpf, C. Näther, and W. Bensch, *Inorg. Chem.*, **38**, 4612 (1999).

6 a) W. Bensch and P. Dürichen, *Chem. Ber.*, **129**, 1207 (1996). b) R. Tillinski, C. Rumpf, C. Näther, P. Dürichen, I. Jeß, S. A. Schunk, and W. Bensch, *Z. Anorg. Allg. Chem.*, **624**, 1285 (1998).

7 a) W. Bensch, P. Dürichen, and C. Weidlich, *Z. Kristallogr.*, **211**, 932 (1996). b) K. O. Klepp and G. Gabl, *Eur. J. Solid State Inorg. Chem.*, **34**, 1119 (1997).

8 S. A. Sunshine, D. Kang, and J. A. Ibers, *J. Am. Chem. Soc.*, **109**, 6202 (1987).

9 a) M. G. Kanatzidis and A. C. Sutorik, *Prog. Inorg. Chem.*, **43**, 151 (1995). b) M. G. Kanatzidis, *Chem. Mater.*, **2**, 353 (1990). c) M. A. Pell and J. A. Ibers, *Chem. Ber.*, **130**, 1 (1997). d) J. Li, H. Y. Guo, D. M. Proserpio, and A. Sironi, *J. Solid State Chem.*, **117**, 247 (1995).

10 a) M. Latroche and J. A. Ibers, *Inorg. Chem.*, **29**, 1503 (1990). b) S. Herzog, C. Näther, and W. Bensch, *Acta Crystallogr.*, **C54**, 1742 (1998).

11 Y. J. Lu and J. A. Ibers, *Comments Inorg. Chem.*, **14**, 229 (1993).

12 H.-W. Ma, G.-C. Guo, M.-S. Wang, G.-W. Zhou, S.-H. Lin, Z.-C. Dong, and J.-S. Huang, to be submitted.

13 a) G.-C. Guo, R. W. M. Kwok, and T. C. W. Mak, *Inorg. Chem.*, **36**, 2475 (1997). b) G.-C. Guo and T. C. W. Mak, *J. Chem. Soc., Dalton Trans.*, **1997**, 709. c) G.-C. Guo and T. C. W. Mak, *Inorg. Chem.*, **37**, 6538 (1998). d) G.-C. Guo and T. C. W. Mak, *Chem. Commun.*, **1999**, 377.

14 Siemens, SHELXTL^{TM} Version 5 Reference Manual, Siemens Energy & Automation Inc., Madison, Wisconsin, 1994, USA.